



## IDENTIFYING NODES AND ANTI-NODES OF A LONGITUDINALLY VIBRATING ROD RESTRAINED BY A LINEAR SPRING IN-SPAN

M. GÜRGÖZE

*Faculty of Mechanical Engineering, Technical University of Istanbul,  
80191 Gümüşsuyu Istanbul, Turkey*

*(Received 22 June 1998)*

Recently, in this journal an interesting study was published [1] which developed a procedure that allows the determination of the location of the nodes and anti-nodes of a complicated structure. The basis of the method is to attach a virtual element (lumped mass or a grounded spring) to the system and to plot the frequency curves of the combined system against the location of the virtual element. It was shown that for virtual lumped mass, the nodes and anti-nodes correspond to the local maxima and minima of the frequency curves, respectively, while for the virtual spring, they correspond instead to the minima and maxima of the frequency curves.

The method is illustrated by examining a uniform cantilevered Bernoulli–Euler beam with various lumped attachments. It is stated, however, that the method is sufficiently general such that it can be easily extended to locate the nodes and anti-nodes of other combined dynamical systems. The aim of this letter is to make a positive comment on this interesting study and to strengthen the authors' statement on the general applicability of their method by giving an example from the field of longitudinally vibrating rods restrained by a linear spring in-span. In an earlier study, the authors also considered a longitudinally vibrating rod, carrying a lumped mass in-span [2]. They applied the virtual mass approach. Here, in contrast, the virtual grounded spring approach will be employed.

The “original” mechanical system to be investigated is shown in Figure 1(a). It consists of a fixed–free longitudinally vibrating elastic rod of length  $L$  and axial rigidity  $EA$  which is restrained by a linear spring of spring coefficient  $k$ . The mass per unit length and location of the spring attachment point are  $m$  and  $\eta L$ , respectively. The aim is to locate the nodes and the anti-nodes of this “original” system. To this end, according to the virtual spring approach, a virtual grounded spring of spring coefficient  $k_1$  is attached to the system as in Figure 1(b) and then, the frequency curves of the resulting “combined” system are plotted against the constraint location parameter  $\eta_1$ . The nodes and anti-nodes of the original system correspond to the local minima and maxima of these curves. Unlike those in reference [1], the calculations here will be based on expressions of the “exact” frequency equations which are derived and given in the appendix.

Figures 2 and 3 illustrate the exact mode shapes of the original system and the dimensionless natural frequency curves of the combined system as a function of the location parameter of the virtual spring attachment point  $\eta_1$ . For brevity, only

the second and third dimensionless frequency curves  $\bar{\beta}_2(\eta_1)$  and  $\bar{\beta}_3(\eta_1)$  are shown, where  $\alpha_k = \eta = 0.5$  are chosen for the data of the original system in Figure 1(a). In both figures, the three values for the dimensionless virtual spring stiffness parameter are  $\alpha_{k_1} = 0.1, 0.5$  and  $1.0$ . The first three roots of the frequency equation (A9) are  $\bar{\beta}_1 = 1.715507$ ,  $\bar{\beta}_2 = 4.764809$  and  $\bar{\beta}_3 = 7.885674$ , respectively, which represent the dimensionless eigenfrequency parameters of the original system. Inspection of Figures 2 and 3 validates the results reached and the observations made from the figures in reference [1] that use other vibrating systems.

From the present figures it can be observed that the locations of the local minima of the frequency curves of the combined system correspond to the nodes of the original system, and that they are independent of the stiffness parameter  $\alpha_{k_1}$  of the virtual spring. Furthermore, the locations of the local maxima of the frequency curves of the combined system which are nearly invariant of  $\alpha_{k_1}$  correspond to the anti-nodes of the original system. It is evident that as  $\alpha_{k_1}$  increases, the frequency curves shift upwards because the overall stiffness of the combined system becomes larger.

From Table 1, it can be clearly seen how well the virtual grounded spring approach locates the nodes and anti-nodes of the original system.

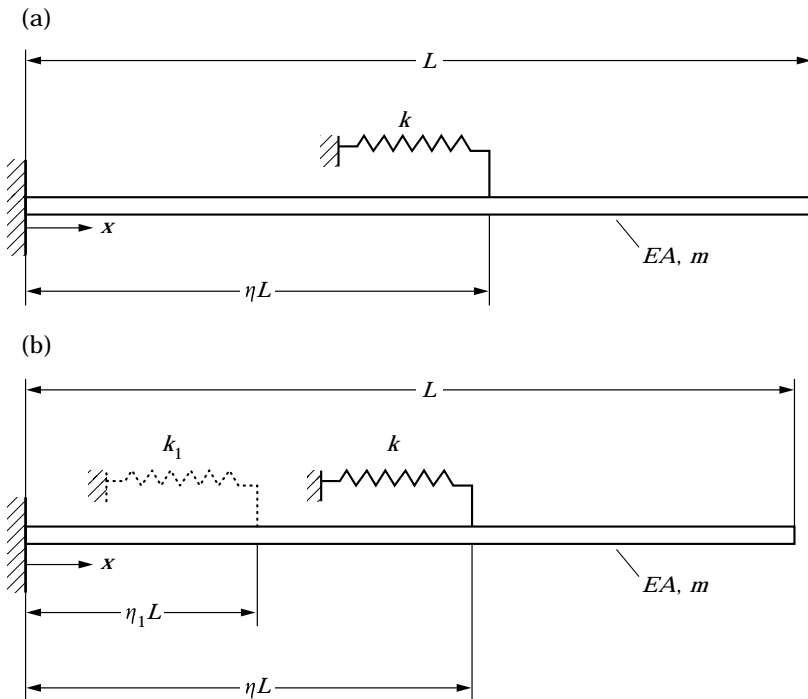


Figure 1(a). Original system: a fixed-free longitudinally vibrating elastic rod, restrained at  $x = \eta L$  by a linear spring of spring coefficient  $k$ . (b) Combined system: original system with a virtual grounded spring attached at  $x = \eta_1 L$ , the spring coefficient of which is  $k_1$ .

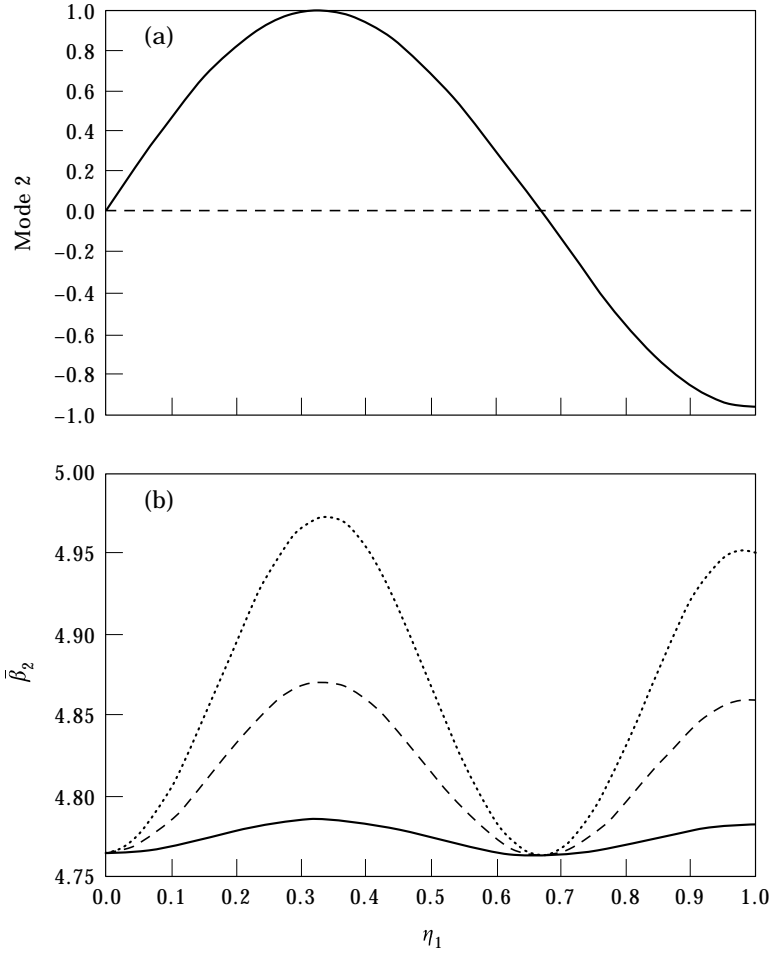


Figure 2(a). Exact second mode shape for the original system in Figure 1(a). (b) The corresponding frequency curves as a function of the location parameter of the attachment point  $\eta_1$  of the virtual spring. —,  $\alpha_{k_1} = 0.1$ , ---, 0.5, . . . . 1.0.

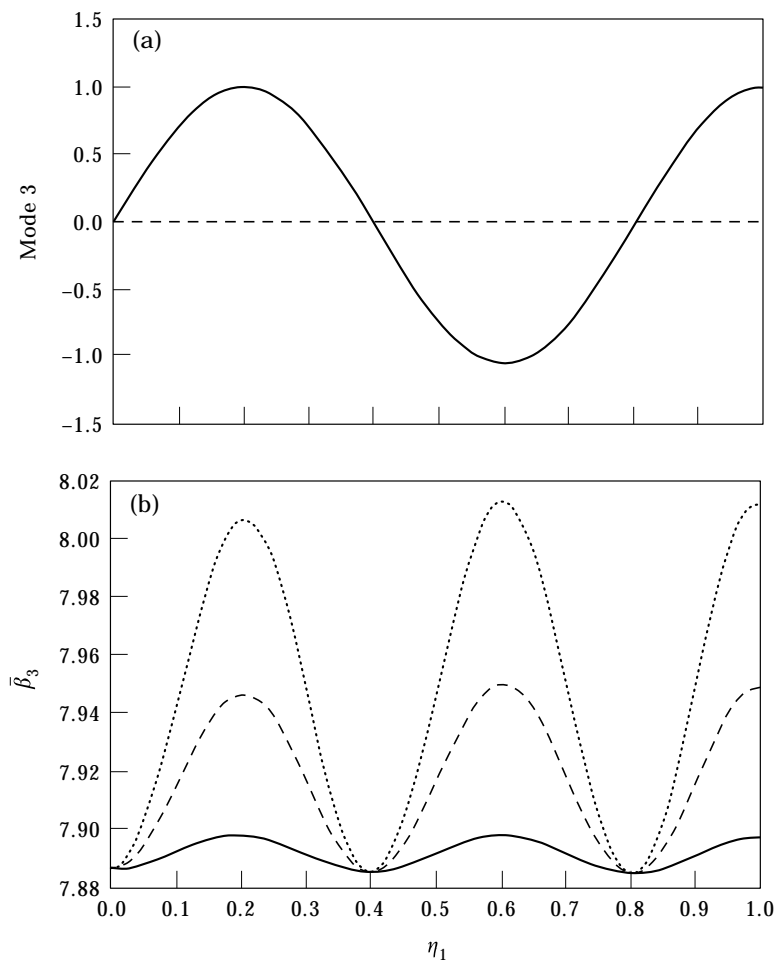


Figure 3(a). Exact third mode shape for the original system in Figure 1(a). (b) As in Figure 2(b).

TABLE 1

*Location of the nodes and anti-nodes of the system in Figure 1(a), for  $\eta = \alpha_k = 0.5$ , determined exactly and by using the virtual grounded spring approach. The subscripts  $n$  and  $an$  denote the "node" and "anti-node", respectively, while the subscripts  $e$  and  $vs$  correspond to "exact" and "virtual spring". Above results are obtained by setting  $\alpha_{k_1} = 0.1$ , where  $\alpha_{k_1}$  represents the dimensionless stiffness coefficient of the virtual grounded spring*

Mode number	$\bar{x}_n^e$	$\bar{x}_n^{vs}$	$\bar{x}_{an}^e$	$\bar{x}_{an}^{vs}$
2	0.670	0.670	0.330	0.330
3	0.398	0.398	0.199	0.200
	0.801	0.801	0.602	0.602

## REFERENCES

1. P. D. CHA, C. L. DYM and W. C. WONG 1998 *Journal of Sound and Vibration* **211**, 249–264. Identifying nodes and anti-nodes of complex structures with virtual elements.
2. P. D. CHA and C. L. DYM 1997 *Journal of Sound and Vibration* **203**, 533–535. Identifying nodes and anti-nodes of an axially vibrating bar with lumped mass.

## APPENDIX

The equations of motion of the three rod-portions of the combined system are the well-known partial differential equations

$$EA \frac{\partial^2 u_i(x, t)}{\partial x^2} = m \frac{\partial^2 u_i(x, t)}{\partial t^2} \quad (i = 1, 2, 3), \quad (\text{A1})$$

where  $u_1(x, t)$ ,  $u_2(x, t)$  and  $u_3(x, t)$  denote the axial displacements of the rod portions  $0 \leq x \leq \eta_1 L$ ,  $\eta_1 L \leq x \leq \eta L$  and  $\eta L \leq x \leq L$ , respectively. The corresponding boundary and matching conditions are,

$$\begin{aligned} u_1(0, t) &= 0, & u_1(\eta_1 L, t) &= u_2(\eta_1 L, t), \\ EAu_1'(\eta_1 L, t) - EAu_2'(\eta_1 L, t) + k_1 u_1(\eta_1 L, t) &= 0, \\ u_2(\eta L, t) &= u_3(\eta L, t), \\ EAu_2'(\eta L, t) - EAu_3'(\eta L, t) + k u_2(\eta L, t) &= 0, & u_3'(L, t) &= 0, \end{aligned} \quad (\text{A2})$$

where primes denote partial derivatives with respect to the position co-ordinate  $x$ . Using the standard method of separation of variables, one assumes

$$u_i(x, t) = U_i(x) \cos \omega t \quad (i = 1, 2, 3), \quad (\text{A3})$$

where  $U_i(x)$  are the amplitude functions and  $\omega$  is the unknown eigenfrequency of the combined system.

Substitution of these into equations (A1) results in

$$U_i''(x) + \beta^2 U_i(x) = 0 \quad (i = 1, 2, 3), \quad (\text{A4})$$

where  $\beta^2 = m\omega^2/EA$ .

Substituting equations (A3) into (A2) yields

$$U_1(0) = 0, \quad U_1(\eta_1 L) = U_2(\eta_1 L),$$

$$EAU_1'(\eta_1 L) - EAU_2'(\eta_1 L) + k_1 U_1(\eta_1 L) = 0, \quad U_2(\eta L) = U_3(\eta L),$$

$$EAU_2'(\eta L) - EAU_3'(\eta L) + kU_2(\eta L) = 0, \quad U_3(L) = 0. \quad (\text{A5})$$

The general solutions of equation (A4) are simply

$$U_i(x) = C_i \sin \beta x + D_i \cos \beta x, \quad (i = 1, 2, 3), \quad (\text{A6})$$

$C_i$  and  $D_i$  being six integration constants to be evaluated via conditions (A5). The application of these conditions to the solutions (A6) yields a set of six homogeneous equations for  $C_1, \dots, D_3$ . A non-trivial solution of this set of equations is possible only if the characteristic determinant of the coefficients vanishes. This condition leads, considering that  $D_1$  vanishes, to the following frequency equation:

$$\left| \begin{array}{ccccc}
\sin \eta_1 \bar{\beta} & -\sin \eta_1 \bar{\beta} & -\cos \eta_1 \bar{\beta} & 0 & 0 \\
\bar{\beta} \cos \eta_1 \bar{\beta} + \alpha_{k_1} \sin \eta_1 \bar{\beta} & -\bar{\beta} \cos \eta_1 \bar{\beta} & \bar{\beta} \sin \eta_1 \bar{\beta} & 0 & 0 \\
0 & \sin \eta \bar{\beta} & \cos \eta \bar{\beta} & -\sin \eta \bar{\beta} & -\cos \eta \bar{\beta} \\
0 & \bar{\beta} \cos \eta \bar{\beta} + \alpha_k \sin \eta \bar{\beta} & -(\bar{\beta} \sin \eta \bar{\beta} - \alpha_k \cos \eta \bar{\beta}) & -\bar{\beta} \cos \eta \bar{\beta} & \bar{\beta} \sin \eta \bar{\beta} \\
0 & 0 & 0 & \cos \bar{\beta} & -\sin \bar{\beta}
\end{array} \right| = 0, \quad (\text{A7})$$

where

$$\bar{\beta} = \beta L, \quad \alpha_k = \frac{k}{EA/L}, \quad \alpha_{k_1} = \frac{k_1}{EA/L}. \quad (\text{A8})$$

It is important to note that equation (A7) is valid for  $\eta_1 \leq \eta$ . In the case of  $\eta_1 > \eta$ , in the determinant,  $\eta_1$  and  $\alpha_{k_1}$  are to be replaced by  $\eta$  and  $\alpha_k$ , respectively, and vice versa.

Having obtained the frequency equation of the more complex system in Figure 1(b), it is an easy matter to show that the frequency equation and the mode shapes of the simpler system in Figure 1(a) are given by:

$$\bar{\beta} \cos \bar{\beta} + \alpha_k \sin \eta \bar{\beta} \cos [(1 - \eta)\bar{\beta}] = 0 \quad (\text{A9})$$

and

$$U_1(\bar{x}) = \sin \bar{\beta} \bar{x} \quad (0 \leq \bar{x} \leq \eta), \quad (\text{A10})$$

$$U_2(\bar{x}) = \left( 1 + \frac{\alpha_k}{2\bar{\beta}} \sin 2\eta \bar{\beta} \right) \sin \bar{\beta} \bar{x} - \frac{\alpha_k}{\bar{\beta}} \sin^2 \eta \bar{\beta} \cos \bar{\beta} \bar{x} \quad (\eta \leq \bar{x} \leq 1),$$

where  $\bar{x} = x/L$  is introduced.